

# Impact of backtracking strategies on techno-economics of horizontal single-axis tracking solar photovoltaic power plants

Dominik Keiner<sup>a,\*</sup>, Lukas Walter<sup>b</sup>, Mai ElSayed<sup>a</sup>, Christian Breyer<sup>a,\*</sup>

<sup>a</sup> School of Energy Systems, LUT University, Yliopistonkatu 34, 53850 Lappeenranta, Finland

<sup>b</sup> Faculty of Electrical Engineering and Information Technology, OTH Regensburg, Prüfening Str. 58, 93049 Regensburg, Germany

## ARTICLE INFO

### Keywords:

Solar photovoltaics  
Single-axis tracking  
Backtracking  
Economic optimisation  
Half-cut solar cell

## ABSTRACT

Optimisation of horizontal single-axis tracking solar photovoltaic power plants is important for its optimal application. Commonly, standard backtracking has been applied to avoid mutual shading and improve the full load hours and levelised cost of electricity; however, this approach is not always the best solution for state-of-the-art modules with half cell technology. Backtracking has not yet been studied for different test sites with different solar and climatic conditions. This study aims to improve the knowledge on the techno-economic performance of horizontal single-axis tracking systems with half cell modules applying different backtracking strategies in full hourly resolution for nine test sites globally and varying row spacing. In addition to the standard backtracking algorithm, an advanced backtracking algorithm that varies the tracking angle only if the irradiance can be improved, and an advanced sophisticated backtracking algorithm simulating the irradiance for all possible tracking angles, are studied. The results confirm that standard backtracking is only superior for specific conditions. Compared to no backtracking, standard backtracking shows up to ca. 9% higher levelised cost of electricity due to lower full load hours. Advanced backtracking can lower the levelised cost of electricity by up to 9% and advanced sophisticated backtracking by up to 12%, due to improved full load hours. In general, results are similar and comparable for all test sites studied. This study highlights the importance of backtracking for optimised future horizontal single-axis tracking system planning.

## 1. Introduction

Solar photovoltaics (PV) is set to be the number one renewable energy source of the 21st century. This fact was set by the International Energy Agency, who have referred to solar PV as the ‘new king’ of power generation in the 2020 World Energy Outlook (WEO) [1]. Indeed, solar PV shows tremendous potential globally for the decades to come [2–4]. Within the growing capacity, tracking systems see a growing interest as well, mainly to their attractive techno-economic performance [5]. Especially, single-axis tracking systems, and, more specifically horizontal single-axis tracking (HSAT) systems, are expected to increase their market share in the utility-scale solar PV installations from about 30% at present to about 40% by 2030 [6,7]. In cost optimised energy system analyses, the market share was found to be able to further grow to about 60% by 2050 [8].

Despite the very good prospects of HSAT systems, HSAT solar PV is rarely used in energy system modelling. Since 2018, when Afanasyeva et al. [9] published the study on the relevance of HSAT solar PV for the

energy transition, many more studies have been published covering the performance of HSAT solar PV with various contexts. Antonanzas et al. [10] studied the optimal tracking strategy for the case of Europe under cloudy conditions. Verissimo et al. [11] optimised the system configuration of HSAT in Brazil, also including backtracking for crystalline silicon (c-Si) modules. Tracking schedules for different weather conditions were subject to a study by Kuttybay et al. [12]. Zhu et al. [13] propose an update of conventional HSAT structure to a tilt-rotation structure for maximising the yield of single-axis tracking systems at different latitudes. However, in recent years, the interest in HSAT systems seems to shift towards the combination of HSAT with bifacial modules [14–16]. Only a few energy system models include tracking solar PV in their energy transition analyses, such as LUT-ESTM [8], GATOR-GCMOM/LOADMATCH [17], and the ANU model [18].

On the module level, half cells are already the leading cell option for c-Si modules with a current market share of about 90% [19], while single-axis tracker systems show a market share of about 36% in utility-scale solar PV power plants [6]. Fig. 1 shows the market shares of cell

\* Corresponding authors.

E-mail addresses: [dominik.keiner@lut.fi](mailto:dominik.keiner@lut.fi) (D. Keiner), [christian.breyer@lut.fi](mailto:christian.breyer@lut.fi) (C. Breyer).

<https://doi.org/10.1016/j.solener.2023.112228>

Received 5 September 2023; Received in revised form 20 October 2023; Accepted 25 November 2023

Available online 15 December 2023

0038-092X/© 2023 The Author(s). Published by Elsevier Ltd on behalf of International Solar Energy Society. This is an open access article under the CC BY license (<http://creativecommons.org/licenses/by/4.0/>).

technologies, market shares of HSAT, and expected total share in solar PV installations estimated based on Bogdanov et al. [8].

Therefore, the combination of half cell modules with single-axis tracking systems can be estimated to be about a third of all solar PV installations globally. Assuming the HSAT installation rates of Bogdanov et al. [8] and the abovementioned market shares of half cell modules and HSAT systems, about 4.4 TW<sub>p</sub> half cells and single-axis tracking system combinations are estimated to be installed between 2023 and 2030, covering a significant share of about 43% of the total global cumulated utility-scale solar PV market in this time frame. Yield optimisation of these systems is indispensable to provide the least cost system solution and could accelerate the energy transition by using renewable energy technology at its best performance.

One, if not the most significant, performance issue of solar PV and HSAT systems is mutual or self-shading of the tracker rows. To avoid self-shading of the trackers, which limits the yield of the solar PV modules, backtracking has been introduced as a viable option to avoid such losses [21]. Most systems and scientific literature apply the standard backtracking first introduced by Panico et al. [22], e.g., Verissimo et al. [11]. The standard backtracking method avoids mutual shading of the trackers, which beneath yield improvement, also reduces the risk of hot spots [21]. While studying further literature (cf. section 2), the lack of a detailed investigation of alternative backtracking strategies for several sites globally with different conditions for half cell modules to investigate the cost-optimal backtracking strategy becomes clear.

This study aims to close this research gap by modelling solar PV HSAT systems to find advantages and disadvantages of different backtracking strategies. The novelties presented in this study are:

- Investigation of several test sites around the globe with different solar and varying climatic conditions.
- Hourly resolved modelling of a solar PV HSAT system.
- Different backtracking strategies investigated.

- Presentation of several techno-economic results for a comparison of the techno-economic performance of the solar PV HSAT system applying the respective backtracking strategy.

The results presented will help in further energy system modelling and planning by including the most suitable backtracking strategy subsequently allowing for a yield, and therefore, cost-optimised energy system especially for high shares of solar PV. Issues and limitations regarding the backtracking strategies shall be discussed.

## 2. Literature review

In this section, scientific literature is reviewed in the context of backtracking applied for solar PV tracking systems with a focus on single-axis tracking systems. In the case of 2-axis tracking systems, backtracking strategies have been analysed for example by Fernández-Ahumada [23]. The findings of the literature review are summarised in Table 1.

While backtracking is discussed in various contexts in literature, a comparative analysis between strategies was only done by Anderson [26], though in the context of sloped terrain. Mostly, standard backtracking has been compared to standard tracking procedure [21,24,25,29]. An interesting comparison was made by Passow et al. [27] by comparing c-Si modules with CdTe and they found, that CdTe showed a better performance for true tracking, i.e., tracking without backtracking, due to the module characteristics. Interestingly, Dolan et al. [28] found that half cell modules performed better in cases of backtracking errors, which means that the avoidance of mutual shading did not work and shading occurred. This finding confirms that a more thorough investigation of backtracking and backtracking strategies of half cell modules is required, as it may be very well possible that standard backtracking is not necessarily the best option for half cells.

This research gap shall be closed with the present study by modelling half cell HSAT systems for different test sites around the world and by applying different backtracking strategies. The results shall show

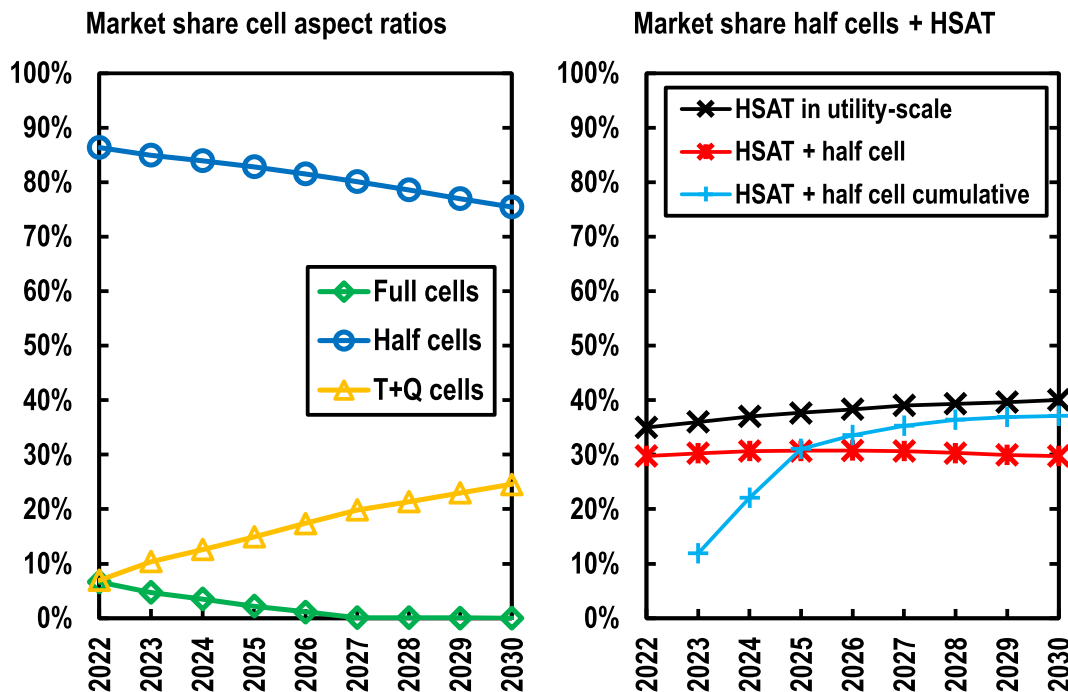


Fig. 1. Market shares of cell aspect ratios (left) and market shares of single-axis tracking systems (HSAT) and combined share in total utility-scale solar PV capacity installations (right) until 2030. Cell technology market shares [19,20], single-axis tracking systems [6], and share of half cell single-axis tracking systems in total and cumulative solar PV installations are based on Bogdanov et al. [8]. Numbers have been obtained by applying interpolation to given values in the sources. Abbreviations: T + Q (third and quarter).

**Table 1**

Relevant literature regarding backtracking for single-axis solar PV tracking in chronological order.

Study	Location	Key findings
Silva et al. [24]	n/a	Standard backtracking results in slightly higher annual electricity yield; fewer shading losses, higher losses due to less optimised orientation
Nicoletti et al. [25]	Cosenza, Italy	Standard backtracking applied for monofacial and bifacial modules; higher yield gain for monofacial modules
Anderson [26]	Goodwin Creek, Mississippi, United States	Different backtracking strategies for cross-axis slope happened to show increased array yield
Passow et al. [27]	California/Arizona, United States	Standard backtracking for c-Si modules was outperformed by cadmium telluride (CdTe) modules applying true tracking
Dolan et al. [28]	San Luis Obispo, California, United States	While applying standard backtracking, half cells showed better performance than full cells during backtracking errors when mutual shading occurs
Ngan et al. [29]	North America, not further specified	True tracking (always following the sun) outperformed standard tracking including backtracking for a specific module
Schneider [30]	n/a	Mathematical derivation of standard backtracking strategy; comparison with fixed-tilted solar PV installations
Lorenzo et al. [21]	Amareleja, Portugal	Backtracking with superior performance; backtracking for 2-axis tracking systems introduced
Panico et al. [22]	n/a	Standard backtracking introduced for the first time in literature

whether backtracking in general, or standard backtracking as applied for full cells is the most optimal solution, and what conclusion can be drawn from a global perspective for modern HSAT systems in the coming years.

### 3. Methods and data

This section presents the model specifications and yield modelling details. As the model is widely applied according to previous solar PV tracker modelling by Afanasyeva et al. [9], this section focuses solely on model updates. Additionally, the applied backtracking strategies, test sites, model validation and economic assessment are presented.

#### 3.1. Modelling of horizontal single-axis tracking systems

In this section, the technical modelling and specifications of the considered HSAT system are presented. This includes the basic solar PV and tracking model, some improvements made to a prior model and shading of solar PV modules.

##### 3.1.1. System specifications

The basic HSAT system modelling is based on Afanasyeva et al. [9]. Some changes have been made to the prior system setup. A Nextracker tracking system is chosen [31], which allows for the installation of up to 120 modules per tracker, or 60 modules in a row in 2-in-portrait (2P) orientation. The 2P orientation has some advantages over landscape orientation or 1-in-portrait (1P) orientation. 2P orientation allows for a higher capacity density compared to landscape orientation, as more modules can be installed per tracker. Furthermore, 2P orientation enables a higher ground cover ratio (GCR), and subsequently, a cost-improved system design. Bifacial modules, which are out of scope of the present study, with 2P orientation combine high capacity density of the tracker and avoidance of backside shading from torque tubes of the tracker due to a possible module gap, thus increasing backside irradiance. A Longi Hi MO 4 series module is chosen, and the inverter is modelled based on a model from Sineng as a utility-scale inverter with multiple maximum power point (MPP) trackers, enabling the best

performance. The technical parameters are listed in Table 2.

The NX Gemini has a tracking or tilt limit of  $\pm 50^\circ$ . Given the mentioned dimensions of the module and gaps, the chosen axis elevation ensures about 0.6 m elevation of the lower part of the modules if the tracker is in the full limit position. This margin avoids shading of the modules from vegetation in front of the tracker. A half cell technology is chosen as the current industry standard with about 90% market share [19]. The inverter is chosen as it has multiple MPP trackers, which enables the most optimal operation of the module strings of each tracker. The sizing ratio of installed solar PV capacity and inverter nameplate capacity is chosen to 1.2 as a good average assumption [34].

##### 3.1.2. Yield modelling

The basic solar PV tracker model including solar irradiance modelling and loss models, except updated equations mentioned in this subsection, are equal to Afanasyeva et al. [9]. Aspects of the model that are not mentioned in this subsection have not been changed and remain the same. Weather data are used for the year 2005 from the NASA [35,36], which have been reprocessed by the German Aerospace Center [37]. The data are in hourly resolution for the whole year. It must be noted that for operational optimisation an hourly resolution might not be sufficient. However, for the analysis presented in this study, hourly resolution can be considered to show a sufficiently significant impact.

As the only change of the methods as described by Afanasyeva et al. [9], the calculation of the module temperature has been updated to the method proposed by Akhsassi et al. [38] as described in Eqs. (1), (2). Values used in the simulation are given in brackets in the following variable description.

$$U_L = U_{L0} + U_{L1} \cdot v_w \quad (1)$$

$$T_{mod} = \frac{U_L \cdot T_a + \left[ \tau \alpha - \eta_{STC} \cdot (1 - \beta_{MP} \cdot T_{STC}) \cdot \left( 1 + \gamma_{MP} \cdot \ln \left( \frac{G_{tot}}{G_{STC}} \right) \right) \right] \cdot G_g}{U_L + \eta_{STC} \cdot \beta_{MP} \cdot \left( 1 + \gamma_{MP} \cdot \ln \left( \frac{G_{tot}}{G_{STC}} \right) \right) \cdot G_g} \quad (2)$$

where  $U_L$  is the linear function of the wind speed influence with two dimensionless factors  $U_{L0}$  (25) and  $U_{L1}$  (5.9);  $v_w$  is the wind speed at

**Table 2**

Technical parameter overview of used system components for the modelled HSAT system.

Component	Parameter	Value	Reference
Tracker	Nextracker NX Gemini		Nextracker [31]
	Architecture	2-in-portrait (2P)	
	Axis orientation	Horizontal North-South	
	Modules per tracker	120	
	Modules in row	60	
	Tilt limit	$\pm 50^\circ$	
	Row spacing	variable	
	Axis elevation	2.25 m	
	Axis offset	0.09 m	
	Axis gap	0.15 m	
Module	Longi Solar Hi-MO 4 LR4-72 HPH 440 M G2		Longi [32]
	Nominal capacity	440 W <sub>p</sub>	
	Nominal efficiency	20.2 %	
	Cell technology	PERC	
	Cell type	Twin half cell	
	Cell amount	72	
	Module length	2.094 m	
	Module width	1.038 m	
Inverter	Sineng Electric CP-1000-B-TL		Sineng [33]
	MPP tracker	12	
	AC output	3-phase	
	Sizing ratio <sup>1</sup>	1.2	

<sup>1</sup> author assumption

module height (axis elevation plus axis offset, cf. Table 2). Furthermore,  $T_a$  is the ambient temperature in °C,  $\tau\alpha$  is the factor for thermal diffusivity (0.8),  $\eta_{STC}$  is the module efficiency at standard test conditions (STC),  $\beta_{MP}$  is the temperature coefficient for the maximum power  $MP$  of the module ( $-0.0035\text{ }^{\circ}\text{C}^{-1}$ ),  $T_{STC}$  is the temperature at STC ( $25\text{ }^{\circ}\text{C}$ ),  $\gamma_{MP}$  is an empiric dimensionless coefficient for the maximum power  $MP$  of monocrystalline silicon modules (0.043),  $G_{tot}$  is the total irradiation,  $G_{STC}$  is the irradiation at STC ( $1000\text{ W/m}^2$ ), and  $G_g$  is the plane of array

irradiation (calculated).

Subsequently, the calculation of the relative efficiency of the module has been updated to the empirical model based on PVGIS by Yordanov [39] as shown in Eqs. (3)–(5):

$$G' = \frac{G_{tot}}{G_{STC}} \quad (3)$$

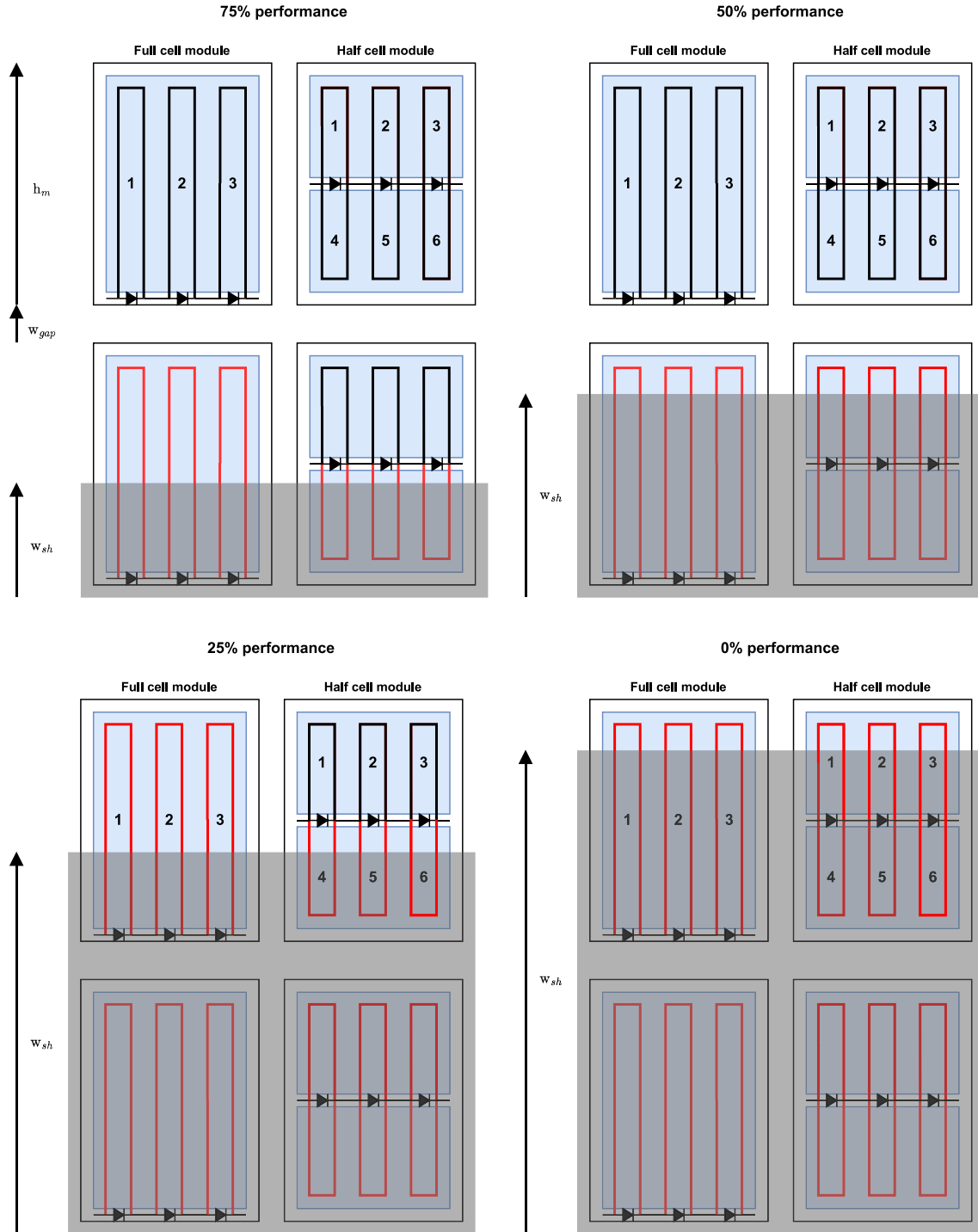


**Fig. 2.** Schematic comparison of sub-string arrangements for full cell modules and half cell modules and assumed tracker performance for horizontal partial shading if the lower block of the lower module is shaded (top left), both blocks of the lower module are shaded (top right), the lower block of the top module is shaded (bottom left), or all blocks are shaded (bottom right) for module setup in portrait orientation. The grey transparent block simulates shading. Red coloured strings indicate bypassed strings due to shading. Black strings indicate normally working strings. Blue areas indicate horizontal module blocks. (For interpretation of the references to colour in this figure legend, the reader is referred to the web version of this article.)

$$T' = T_{mod} - T_{STC} \quad (4)$$

$$\eta_{rel} = 1 + k_1 \bullet \ln G' + k_2 \bullet (\ln G')^2 + T' \bullet [k_3 + k_4 \bullet \ln G' + k_5 \bullet (\ln G')^2] + k_2 \bullet (T')^2 \quad (5)$$

where  $k_1$ - $k_6$  are model coefficients.  $k_1$  and  $k_4$ - $k_6$  are taken from the results given by Yordanov [39].  $k_2$  is chosen to its theoretical value, as validation tests showed better matching results.  $k_3$  is set to be equal to  $\beta_{MP}$ .

Due to the updated assumption of half cell modules that show a different cell string design, the shading model must be adapted because of the different substring arrangement done in half cell modules, as shown in Fig. 2. The applied block model is a particular case of the model by Martínez-Moreno et al. [40].

The substring arrangement allows for six substrings instead of three for half cell modules compared to conventional full cell modules. By splitting the substrings, the top three substrings are still able to deliver electricity in case the lower substrings are shaded. For conventional full cell modules, no substring is able to perform accordingly. Therefore, for horizontal partial shading in portrait orientation, half cell modules show a better performance, since 50% of the substrings can work normally. Considering a 2P orientation where two modules are placed vertically, the tracker can be divided in four blocks. The performance of the whole tracker is then assumed in four steps:

- If the length of the mutual shading  $w_{sh}$  is less than half a module height  $h_m$  of the lower module, the tracker performance is set to 75%.
- If it is more than one module height and less than one module plus the module gap  $w_{gap}$  between the two modules, the tracker performance is set to 50%.
- If the mutual shading covers also parts of the lower half of the upper module, the tracker performance is 25%.
- If all four module blocks are fully or partially shaded, the tracker performance is 0%.

Otherwise, if no mutual shading occurs, the tracker performance is 100% of the possible yield. As a large utility-scale solar PV power plant is presumed, mutual shading is considered for the full tracker length. Further electrical effects of partial shading, as well as edge effects of the power plant are not considered for simplification. The length of the shadow  $d_{sh}$  is calculated by Eq. (6):

$$d_{sh} = h_{col} \bullet \left( \cos(|\beta|) + \frac{\sin(|\beta|)}{\tan(90 - \beta_{true})} \right) \quad (6)$$

where  $h_{col}$  is the height of the column, including two modules and the axis gap,  $\beta$  is the tracking angle, and  $\beta_{true}$  is the true tracking angle. With the length of the shadow, it is possible to calculate the length of mutual shading  $w_{sh}$  as in Eq. (7):

$$w_{sh} = \frac{d_{sh} - d_{row}}{180^\circ - |\beta|} - |\beta_{true}| \bullet \sin(|\beta_{true}|) \quad (7)$$

where  $d_{row}$  is the row spacing of the trackers. The losses of irradiance by shading are then calculated with a factor based on the tracker performance as described above. For the sake of simplicity, it is assumed that yield losses due to tracker performance equals electric losses. The irradiation on the modules after considering shading  $I_{sh}$  is calculated with Eq. (8)

$$I_{sh} = I_{glob} \bullet f_{sh} \quad (8)$$

where  $I_{glob}$  is the global irradiation prior to considering mutual shading, and  $f_{sh}$  is the factor for tracker shade performance.

Inverter efficiency curves are taken from the PVsyst software [41]. The respective efficiency is obtained by doing an interpolation of the

efficiency over relative input power of the inverter. In addition to the new inverter efficiency curves, the dependency of the nominal power of the inverter to the ambient temperature  $T_a$  is included as well. According to available data in PVsyst, the nominal power increases by a factor of 1.1 for  $T_a \leq 25^\circ\text{C}$ . Between  $25^\circ\text{C}$  and  $50^\circ\text{C}$ , the factor decreases from 1.1 to 1.0. Between  $50^\circ\text{C}$  and  $60^\circ\text{C}$ , the factor decreases to 0.9, and between  $60^\circ\text{C}$  and  $65^\circ\text{C}$  the factor decreases to 0 and stays as such for  $T_a \geq 65^\circ\text{C}$ . The factor is obtained by linear interpolation for  $T_a$ .

Furthermore, albedo data are updated to an hourly gridded database [42]. The full yield modelling flow and further calculations can be found in Afanasyeva et al. [9]. Input data, methods for calculations of angles and incident irradiation, soiling and reflection losses, stay unchanged and are implemented according to the prior solar PV single-axis tracker model.

### 3.2. Applied backtracking strategies

In this study, four backtracking strategies are investigated. The strategies given in Table 3 are applied to the tracker yield modelling at every hour of the year. The computation time might be of interest if many nodes were investigated, however, less relevant for single test sites. Due to improvements for computation time, the strategies only consider the irradiance of the modules and do not estimate the electricity output. Since irradiation and electricity yield are directly correlated, this approach is assumed to be valid.

The reference case for the assessment of the effectiveness of the backtracking strategies is the NO strategy. If the sun's elevation is very low, the tracker stays in the tracking limit ( $\pm 50^\circ$ ), without adapting the tracking angle  $\beta$ . Without applying any backtracking, this strategy is the fastest algorithm. The STD modelling algorithm checks whether mutual shading occurs or not. If mutual shading is the case, the tilt is lowered in  $1^\circ$  steps until there is no mutual shading. The minimum tilt angle is  $0^\circ$  corresponding to a horizontally tilted tracker. This strategy still allows for a fast computation due to simple calculations. The ADV strategy checks for the total irradiation on the module instead of mutual shading, which means that, instead of focusing on mutual shading, the algorithm calculates the total irradiation of the current tilt angle and of a  $1^\circ$  lower tilt angle. After comparison, the tilt angle is only reduced if the total irradiation of the module at the reduced angle is higher than of the current angle. This algorithm finds the optimal tilt angle considering the total irradiation on the module surface, which might be found at lower tilt angles in cloudy conditions and a high diffuse component of the irradiation. This strategy neglects shading losses and incidence angle (incidence angle modifier, IAM) losses. Therefore, the computation speed is reduced, as the calculation of the total irradiance even by neglecting some aspects still takes some time. For the ADVS strategy, the irradiation of the module is calculated for all angles between the true

**Table 3**

Explanation of applied backtracking strategies.

Name	Short name	Explanation	Computation speed	Strategy classification
No backtracking	NO	Reference case	Very fast	n/r
Standard backtracking	STD	Reduction of tilt angle until no mutual shading	Fast	Backtracking
Advanced backtracking	ADV	Reduction of tilt angle only if total irradiance can be improved	Fast/Medium	Backtracking + yield optimisation
Advanced sophisticated backtracking	ADVS	Simulation of irradiance at all tilt angles < true tracking angle for global optimum	Slow	Yield optimisation



tracking angle  $\beta_{true}$  and  $0^\circ$  (horizontal orientation) for all hours of the year. The algorithm then chooses the angle with the highest irradiance. An orientation of the tracker to the opposite side less than or bigger than  $0^\circ$ , depending on the starting tracking angle, is not considered, as it is assumed that a module facing away from the sun does not bring any yield improvement. At  $0^\circ$  the best yield occurs on fully cloudy days for maximum diffuse light irradiation. This also improves the simulation speed by avoiding unnecessary calculation steps. This strategy also includes shading and IAM losses. The algorithm finds the global optimum of all possible tilt angles and is therefore, the most sophisticated; thus, one drawback is the relatively long computation time.

Even though all strategies are called backtracking strategies, the classification of the strategies transitions from typical backtracking to yield optimisation the more sophisticated the strategies become. While the STD and ADV strategies take  $1^\circ$  steps for the tilt angle back to achieve the result anticipated with the strategy, the ADVS strategy does not solely deal with the avoidance of shading but is rather optimising the orientation of the modules for an optimised yield. Nevertheless, the wording backtracking is used throughout this study for all strategies, as even the ADVS strategy will result in lower tracking angles as it would be necessary for the given sun elevation at some points.

Flow charts for the three strategies applying backtracking (STD, ADV, ADVS) are shown in the appendix in Figs. A1–A3. As mutual shading also depends on the row spacing, the investigation is made for row spacings between 6 m and 16 m in 1 m steps. While a minimum of 6 m is assumed to allow for maintenance vehicles to access the trackers, 16 m is chosen as the double row spacing of prior single-axis tracker modelling [9].

### 3.3. Test sites and model validation

The performance of the backtracking strategies is studied for nine test sites in different locations around the globe, as shown in Fig. 3.

The test sites are chosen due to their variety of different climatic conditions allowing for a respective model validation (cf. subsection 3.4). Geographic and climatic details for the test sites are given in Table 4.

The test sites cover different types of conditions, from northern sites

with low irradiance and low average temperature (Lappeenranta, Watson Lake), relatively high irradiance and relatively low average temperature (Xilin Gol, Munich), average irradiance and high average temperature (Brasilia, Kuala Lumpur), to high irradiance and high average temperature (Jaisalmer, Tete). The Köppen classification [43,44] also shows a high variety of possible test sites with extreme cases of subarctic to hot desert sites. Effects of climate change on meteorologic input data, such as change in temperature, are not considered in this study.

The solar PV single-axis tracking model used in this study, comprising of existing single-axis tracking modelling [9] and improvements presented in this study, shall furthermore be called LUT-PV. To validate the performance of the LUT-PV model, the test sites have been modelled with PVsyst version 7.3 [41] for comparison. PVsyst offers two options for backtracking: Applying backtracking in general, and irradiance optimisation. The detailed methodology of the options is not explained in the model documentation. Therefore, LUT-PV is validated with the reference case of NO backtracking strategy, as the strategy is clear for this option. The outcome of the model validation is presented in subsection 3.1.

### 3.4. Economic assessment

Besides the technical performance of the HSAT system applying different backtracking strategies, an economic assessment of the impact shall be done as well. Economic input data for HSAT systems, including all auxiliary costs of the tracker, module, inverter, cabling, transformer, etc. up to the point of grid connection are given in Table 5.

For this study, values for 2025 are chosen as the nearest datapoint and representative year for HSAT half cell installations until 2030. The different backtracking strategies are assumed to not incur additional cost for auxiliary devices.

The economic performance is investigated by calculation of the levelised cost of electricity (LCOE) for each backtracking strategy and row distance applied according to Eqs. (6), (7).

$$LCOE = \frac{(CAPEX \cdot crf + OPEX_{fix})}{FLH} + OPEX_{var} \quad (6)$$

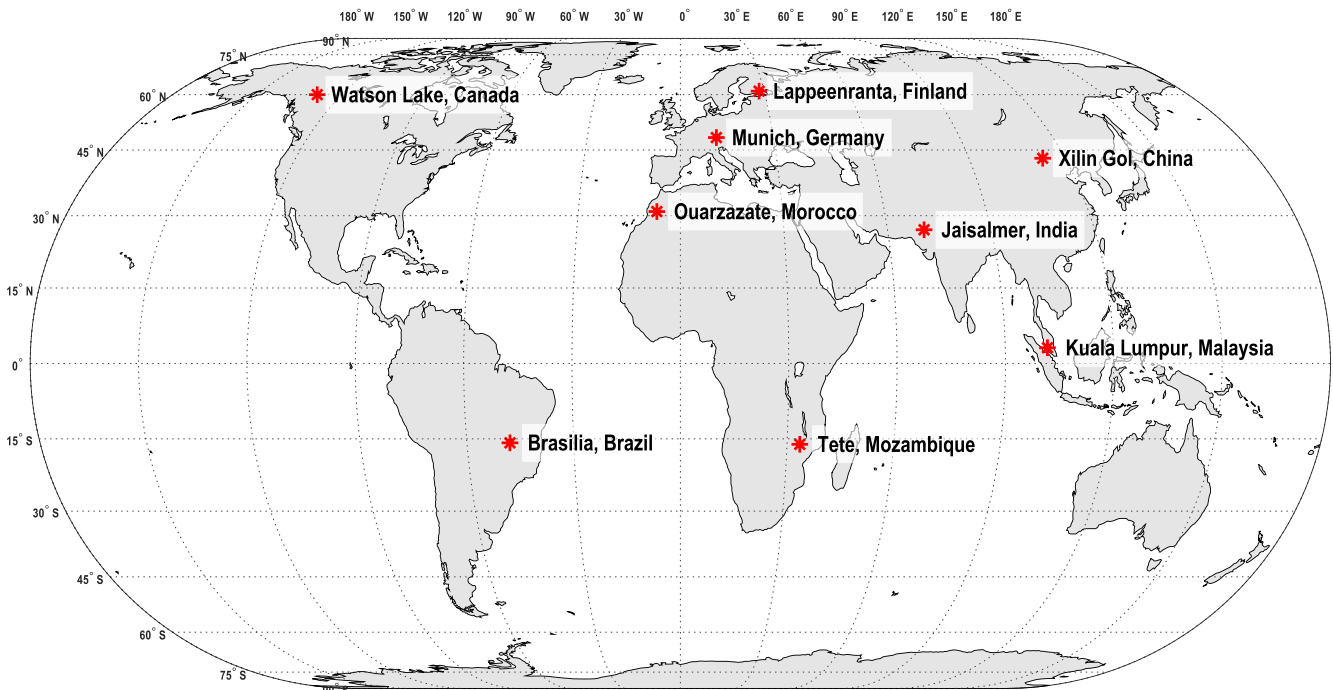


Fig. 3. Map of the locations of the nine test sites considered in this study.

**Table 4**

Specifications of the test sites assessed in this study.

Location	Country	Latitude	Longitude	GHI <sup>1</sup> [kWh/(m <sup>2</sup> •a)]	Average T <sub>a</sub> [°C]	Köppen climate classification [43,44]
Lappeenranta	Finland	61.1° N	28.2° E	983.2	4.8	subarctic / warm summer humid continental
Ouarzazate	Morocco	30.9° N	6.9° W	2024.8	15.2	hot desert
Brasilia	Brazil	15.8° S	47.9° W	1856.9	24.5	tropical savanna with dry winter
Xilin Gol	China	43.0° N	113.0° E	1550.0	6.4	cold semi-arid
Jaisalmer	India	27.0° N	70.6° E	1905.6	29.3	hot desert
Kuala Lumpur	Malaysia	3.1° N	101.7° E	1884.9	28.8	tropical rainforest
Munich	Germany	48.1° N	11.6° E	1100.3	8.6	warm summer humid continental
Watson Lake	Canada	60.0° N	128.7° W	1016.8	−1.5	subarctic
Tete	Mozambique	16.1° S	33.6° E	2026.1	27.0	hot semi-arid

<sup>1</sup> Global horizontal irradiation**Table 5**

Economic input data of the single-axis tracking solar PV system setup for the year 2025. Source: [8].

Parameter	Abbreviation	Unit	Value
Capital expenditure	CAPEX	€/kW <sub>p</sub>	513
Fixed operational expenditure	OPEXfix	€/kW <sub>p</sub> •a	13
Variable operational expenditure	OPEXvar	€/kW <sub>hel</sub> •a	0
Lifetime	N	a	35
Weighted average cost of capital	WACC	%	7

$$crf = \frac{WACC \cdot (1 + WACC)^N}{(1 + WACC)^N - 1} \quad (7)$$

where *crf* is the capital recovery factor and *FLH* are the full load hours achieved by the system. The calculation of the LCOE does not consider the degradation of the modules [45,46], as a rather complex and site-dependent effect. Additionally, solar brightening effects as mentioned by Wild [47], Wild et al. [48], or Fuzzi et al. [49] is worth mentioning as well, though is not part of the economic assessment as of now.

#### 4. Results

Results are presented for the validation of the model, the technical performance regarding yield or FLH of the HSAT system with different backtracking strategies, as well as the impact of the backtracking strategies on the economic performance of the HSAT system. Numeric results for all test sites, row spacings, and backtracking strategies can be found in [Supplementary Material Note 1](#). Numeric results include FLH, LCOE, and relative performance of the backtracking strategies versus the NO and STD strategies. The full set of tracking angle profile graphs can be found in [Supplementary Material Note 2](#).

##### 4.1. Validation results

As already mentioned, the HSAT system has been modelled with PVsyst version 7.3 for comparison and to allow for a validation of the LUT-PV model when applying the reference strategy NO. [Fig. 4](#) shows the achieved system FLH of both models and the relative deviation of the results.

In general, the results are very close. However, LUT-PV tends to slightly overestimates the yield of the HSAT system for most of the test sites, except Kuala Lumpur. Nevertheless, the highest deviation of about 2.5% in Ourzazate (Morocco) is well within an acceptable range. The lowest deviation can be noticed for Munich (Germany) at 0.3%. The average deviation of all test sites is 1.4%. Therefore, LUT-PV can be assumed to deliver valid simulation results.

##### 4.2. Yield performance and shading losses

The yield performance is analysed with the FLH that the HSAT system can achieve. The FLH include all losses considered from the module level, as well as the system level up to the point of grid connection. In [Fig. 5](#), the FLH of the test sites for the four backtracking strategies and different row spacings are shown.

Especially for small row spacings, the STD strategy is clearly worse in yield performance than the reference NO strategy. On the contrary, both the ADV and ADVS strategies can improve the yield compared to the NO strategy by applying some sort of yield optimisation. However, in some cases, the STD strategy shows worse performance for small row spacings and turns into a better option compared to the NO strategy for higher row spacings. This effect might be explained by the reduced backtracking requirement for a bigger row spacing, as mutual shading is naturally reduced by higher distances between the modules. [Table 6](#) shows an overview of average performance of the backtracking strategies.

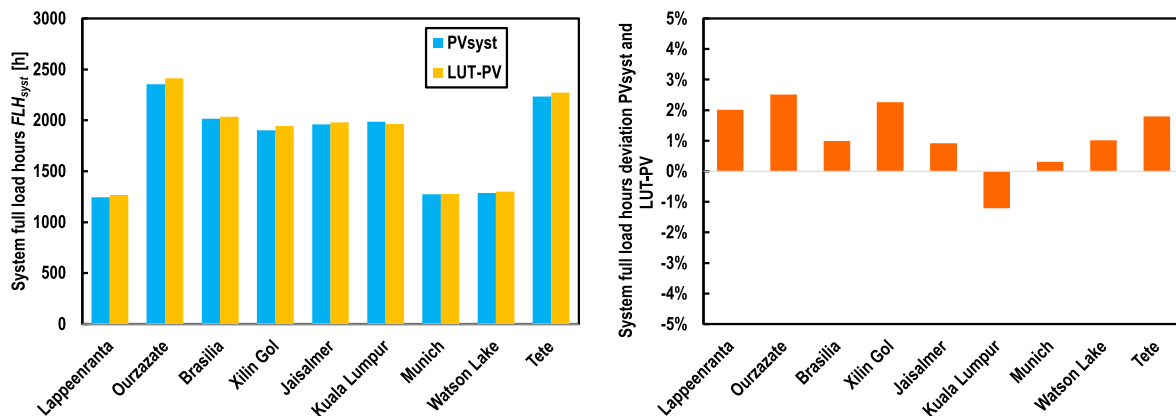


**Fig. 4.** Validation results for monofacial HSAT system and no backtracking. Comparison of the annual system FLH (left) and relative difference of the LUT-PV FLH results with the PVsyst FLH results (right). System FLH specify the FLH of the whole system upon point of grid connection.

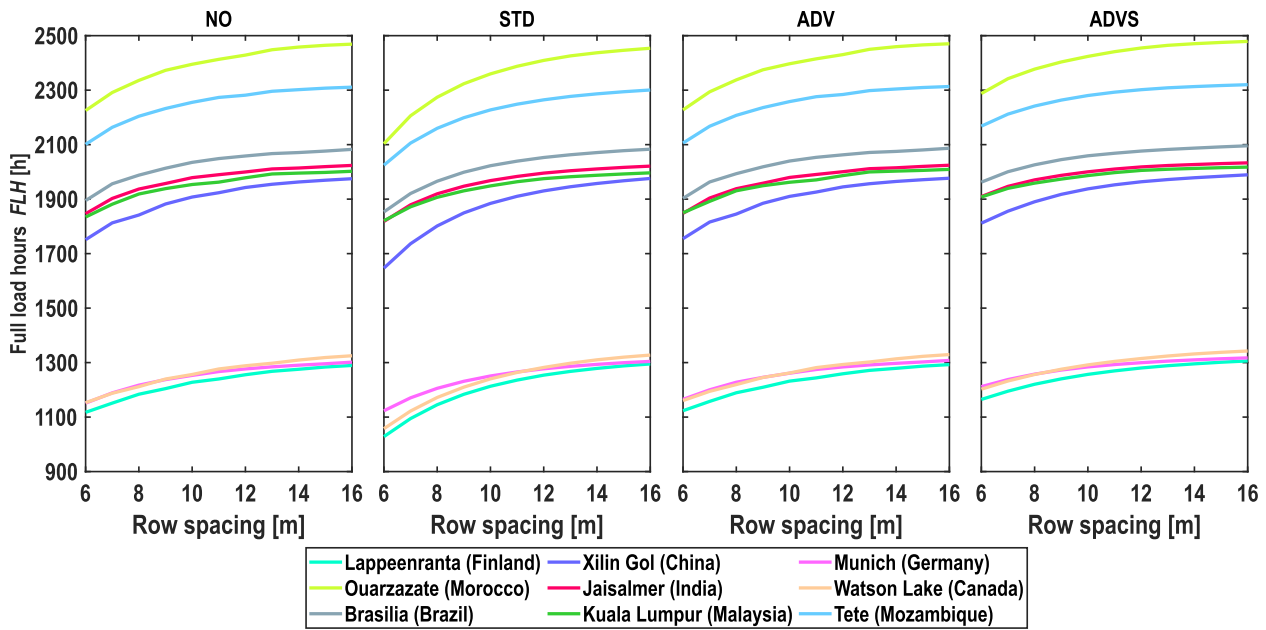


Fig. 5. Results for the technological performance of the HSAT system expressed by FLH of the system. Presented are the four different investigated backtracking strategies NO (left), STD (middle left), ADV (middle right), and ADVS (right) over different row spacings.

Table 6

Average performance of backtracking strategies to no backtracking and row spacing when the underperformance of the backtracking strategy changes to an overperformance.

Test site	Average performance change [%]			Over-/underperformance changes at row spacing [m]		
	STD	ADV	ADVS	STD	ADV	ADVS
Lappeenranta (Finland)	-1.7	0.4	2.4	13	-	-
Ouarzazate (Morocco)	-1.9	0.1	1.2	-	-	-
Brasilia (Brazil)	-0.7	0.1	1.2	14	-	-
Xilin Gol (China)	-1.6	0.1	1.6	16	-	-
Jaisalmer (India)	-0.5	0.1	1.3	-	-	-
Kuala Lumpur (Malaysia)	-0.4	0.5	1.7	-	-	-
Munich (Germany)	-0.4	0.7	2.5	12	-	-
Watson Lake (Canada)	-2.0	0.4	2.6	13	-	-
Tete (Mozambique)	-1.4	0.1	1.2	-	-	-

On average, the STD strategy is not able to improve the system output for any of the test sites. In five cases, the STD changes to a better option compared to the NO strategy for increased row spacing. Therefore, the STD strategy only seems to be sufficient if it is applied in a limited way. Forcing the modules to a significantly different tilt angle during shading also leads to higher incident angles, and therefore, higher reflection and irradiation losses. Due to the improved horizontal shading performance of the half cell modules, partial shading seems therefore to be the lesser evil if parts of the modules can work with better incident angles, even though parts of the module are shaded.

The ADV strategy can improve the system output in every case, though only minorly. The algorithm only increases the tilt angle of the tracker for improved irradiance. As soon as a better angle is found, the algorithm stops. As a result, the algorithm only improves the losses due to the incidence angle and looks for the tilt angle, which allows for the same shading situation, though better incidence angle performance. This effect is shown to be of minor relevance.

On the contrary to the ADV strategy, the ADVS strategy also considers different shading situations. A quick modelling of the situation for all tilt angles between the true tracking angle and  $0^\circ$  allows the algorithm to choose the absolute best angle possible. On average, the yield

improvement is always more than 1%. For small row spacing, which will be necessary for optimising the GCR and the respective area demand for solar PV in the future, this effect is even more significant. The yield improvement can be as high as 5.3% for 6 m row spacing in Munich, Germany. Increasing the row spacing also reduces the advantage of the ADVS strategy and ranges between 0.4% in Tete (Mozambique) and Ouarzazate (Morocco), and 1.3% in Lappeenranta (Finland) and Watson Lake (Canada).

The relative shading losses for the different backtracking strategies are shown in Fig. 6.

The STD strategy can completely avoid all shading losses, as the strategy is designed to do so. Nevertheless, as prior results showed, such a strategy might not always be the solution for the annual yield, as forcing the modules to a significantly lower tilt angle also reduces the irradiation due to a worse incidence angle. The ADV strategy only minorly improves the shading losses. This outcome is interesting, as the algorithm completely ignores the shading losses of the module and only improves the theoretical irradiation on the module by adapting the tilt angle. After the tilt angle is set, no further improvement is done to avoid shading. Still, even though the improvement is minor compared to no backtracking, the ADV strategy has a positive effect, as shown for both the FLH and shading. Such an effect occurs because the ADV strategy applies lower tilt angles at some point when theoretically shading would occur. However, if a lower tilt angle is better due to diffuse light, shading is avoided naturally. The ADVS strategy seems to apply a compromise between allowing shading and minimising shading losses. While the improvement is more significant in absolute numbers for low row spacings, the relative reduction is similar for all row spacings and test sites. On average, the shading is reduced to about 50 % compared to no backtracking. Thus, a conclusion can be drawn that a stringent avoidance of shading for yield improvement is not the best option for HSAT systems applying backtracking.

#### 4.3. Tracking characteristics

To draw conclusions on the reasons for the performance of the different backtracking strategies, the tracking characteristics, i.e., the tracking angle profiles for the strategies, are analysed. Fig. 7 shows the exemplary tracking angle profiles for Lappeenranta, Finland, as a test



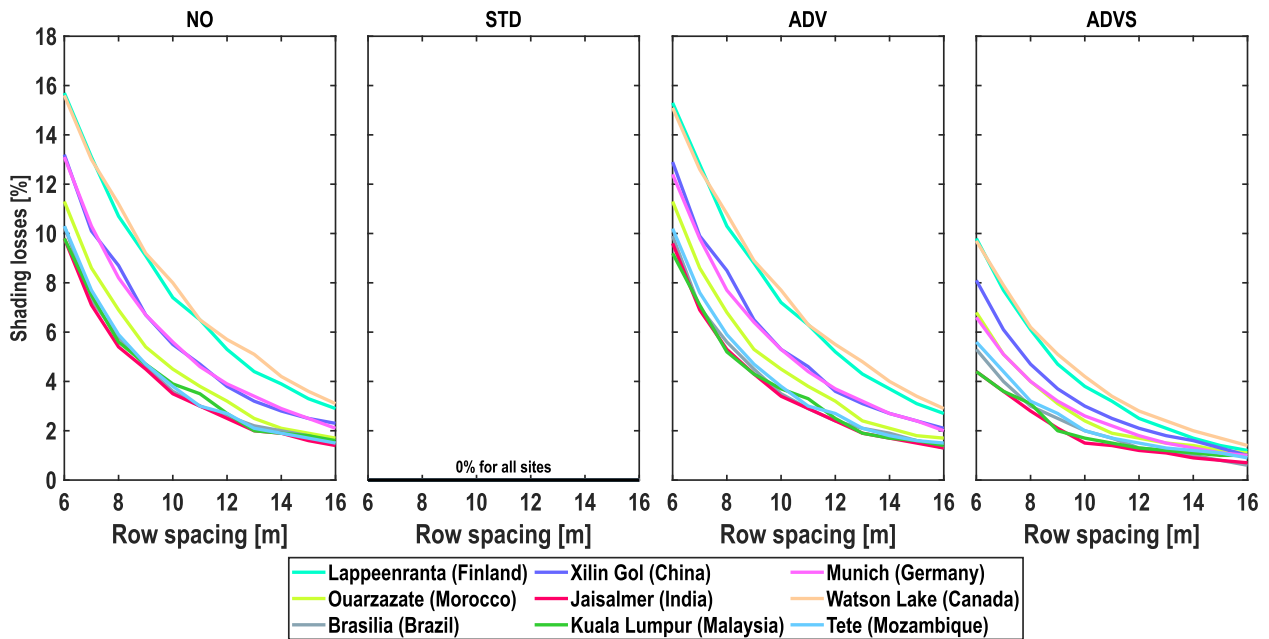


Fig. 6. Shading losses of the solar PV HSAT system relative to the incoming irradiance. Presented are the four different investigated backtracking strategies NO (left), STD (middle left), ADV (middle right), and ADVS (right) over different row spacings.

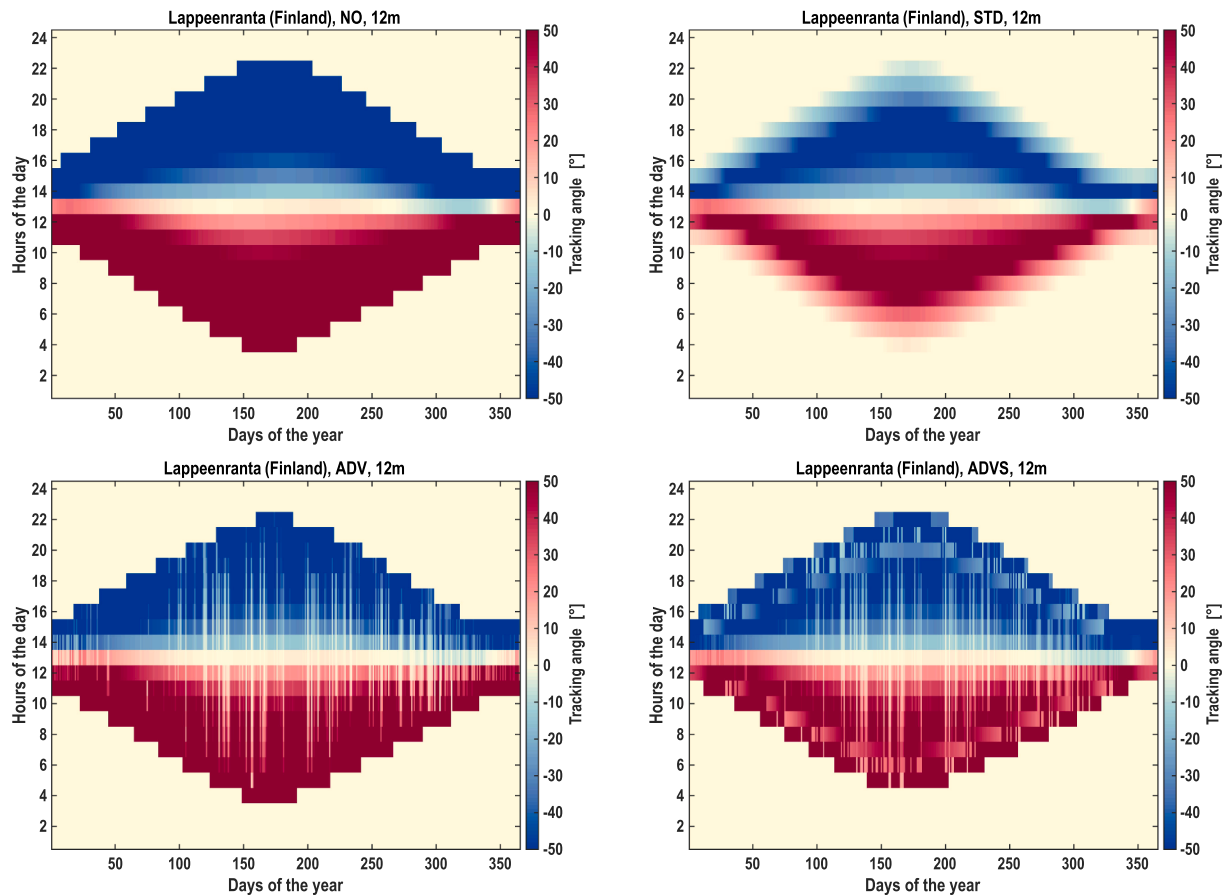


Fig. 7. Tracking angles of all hours of the year for the test site in Lappeenranta (Finland) at 12 m row spacing. Presented are the four applied backtracking strategies NO (top left), STD (top right), ADV (bottom left), and ADVS (bottom right). Steps are due to hourly resolution of the simulation.

site with high seasonality. Per default the modules were assumed to be placed horizontally if the sun is below the horizon during night times.

No detailed explanation is required for the NO strategy. As soon as the sun is below the tracking limit, the tracker stays at this limit. For the

STD strategy, the backtracking in morning and evening times can clearly be seen. In the morning, the tracker starts with tracking angles close to  $0^\circ$ , goes then to the tracking limit and follows the sun during the day. In the evening, the tracking limit is reached first, then the tracking angle is

reduced gradually to avoid mutual shading. By neglecting shading, this effect cannot be seen for the ADV strategy; however, the irradiance optimisation leads to the result that at some days, instead of tracking the sun, the modules are kept at lower tracking angles. These times are most likely those with high cloud coverage and diffuse irradiation share. Even though mutual shading occurs in the mornings and evenings, this optimisation already improves the total annual yield, though minorly. Finally, the most complex tracking angle pattern can be seen for the ADVS strategy as a combination of the NO, STD, and ADV strategies. During the day, tracking angle optimisation is done similarly to the ADV strategy. Shortly after sunrise or right before sunset, the tracking angle is very often kept at high levels, most probably due to higher irradiance for most parts of the modules with better incidence angles, which outweighs the shading losses. Nevertheless, the strategy appears to apply backtracking as soon as the sun is at a relatively high elevation, which occurs about 2 h after sunrise and before sunset. In this case, avoiding mutual shading is the superior strategy for irradiance improvement. In Fig. 8, the tracking characteristics for a test site with almost no seasonality are shown.

Compared to the tracking characteristics shown in Fig. 7 for a high seasonality test site, Fig. 8 shows that only a small difference is noticeable for the STD and ADV strategies. The STD strategy avoids mutual shading, whereas the ADV strategy optimises the tracking angle for total irradiance. However, for the ADVS, the backtracking is much closer to the ADV strategy. While the tracking angle is still chosen to be the tracking limit for early morning and late evening hours in most cases, the backtracking 2 h after sunrise and before sunset is less distinctive in the case of Tete (Mozambique), though still noticeable. As this test site is closer to the equator, the sun rises and sets much faster than high latitude sites. Therefore, in hourly resolution, the ADVS strategy does not

have to apply the backtracking at these times as intensively as shown for the test site in Lappeenranta (Finland).

#### 4.4. Economic performance

A cost-optimised energy system requires optimised system components. The impact of the backtracking strategies on the economics of the HSAT solar PV plant can be assessed by analysing the LCOE of the system and its respective deviations. The LCOE of the HSAT system for the nine test sites are shown in Fig. 9.

The biggest impact on the LCOE is again clearly noticeable for the STD strategy and small row spacings; however, the absolute cost reduction for increasing row spacing is also most evident for the STD strategy. All other strategies perform significantly better for small row spacings than the STD strategy. This result is most interesting in the case of the NO strategy, i.e., that keeping the modules in tracking limit position increases shading. However, forcing the modules in significantly lower tilt angles to avoid mutual shading also significantly lowers the yield of the non-shaded parts of the module due to non-optimal incidence angles, which has a major impact on the overall yield performance in such situations. As has been shown in subsection 3.2 and Table 5, this situation changes at some point, when the STD strategy becomes the superior strategy for increasing row spacings. However, by applying the right backtracking strategy, achieving a LCOE of ca. 40 €/MWh in Lappeenranta, Munich, and Watson Lake is possible as early as 2025, and even to about 45 €/MWh in Munich and Watson Lake for the minimum row spacing. Similar results are possible for the STD strategy only by increasing the row spacing by about 4 m, which can already have a significant effect on the GCR and power density of the power plant. For large row spacings, the difference in LCOE almost vanishes for the four

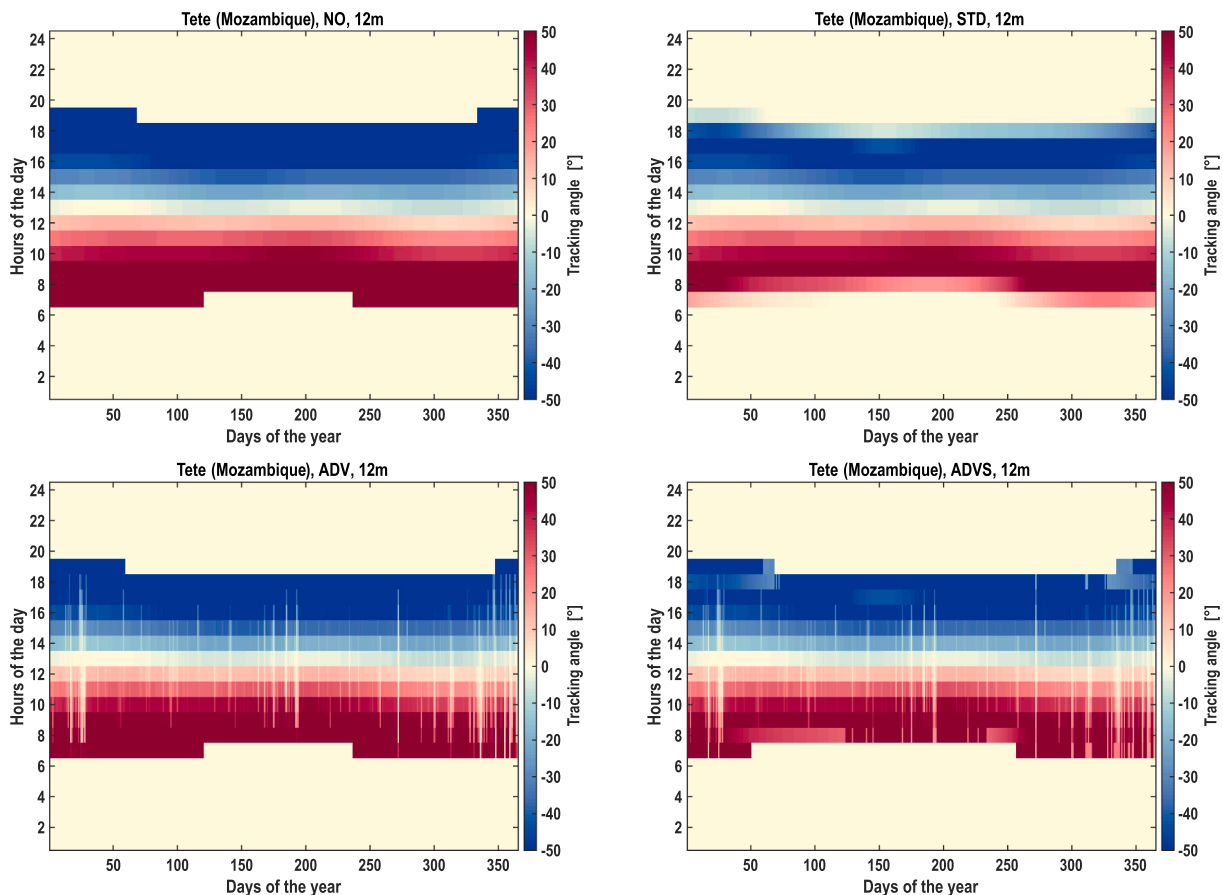


**Fig. 8.** Tracking angles of all hours of the year for the test site in Tete (Mozambique) at 12 m row spacing. Presented are the four applied backtracking strategies NO (top left), STD (top right), ADV (bottom left), and ADVS (bottom right). Steps are due to hourly resolution of the simulation.

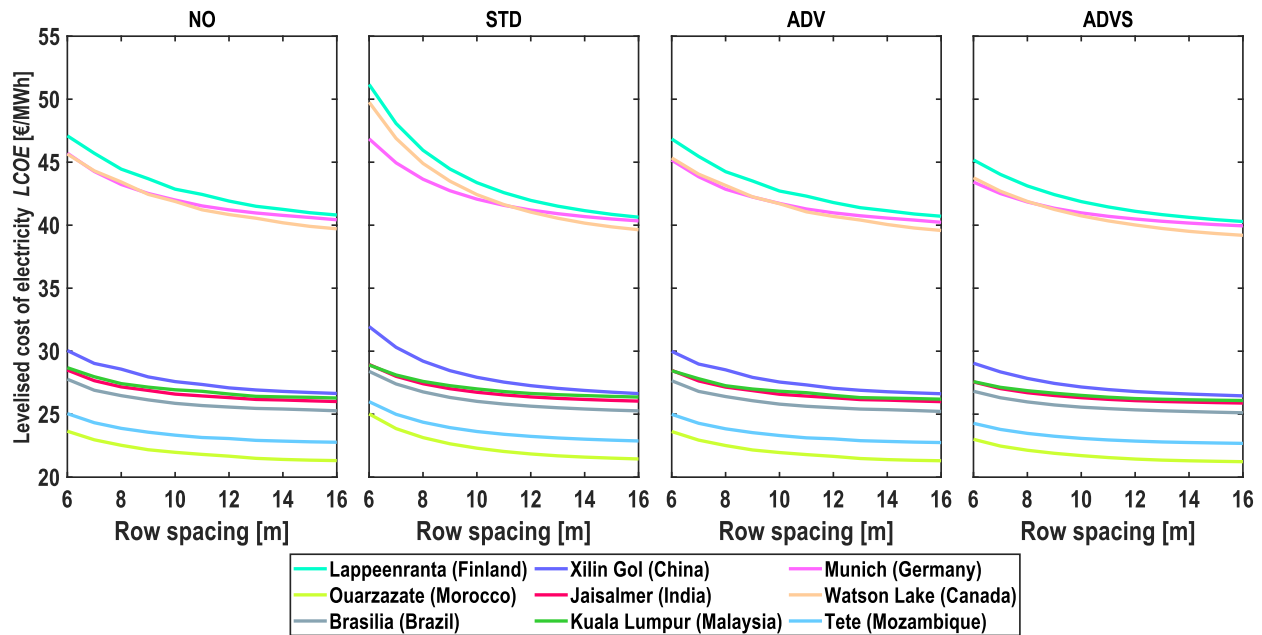


Fig. 9. Results for the economic performance of the HSAT system expressed by LCOE of the system in 2025. Presented are the four different investigated backtracking strategies NO (left), STD (middle left), ADV (middle right), and ADVS (right) over different row spacings.

backtracking strategies, since with bigger row spacing, mutual shading is less eminent and, therefore, the necessity of a sophisticated backtracking strategy is lessened. Interestingly, similar LCOEs are already possible within the investigated row spacing of up to 16 m for the test sites in high latitudes.

Fig. 10 shows the relation of relative LCOE of the strategies vs NO strategy over the relative relation of FLH and the range of relative LCOE for each of the nine test sites, as well as the relative LCOE of the strategies compared to the STD strategy and LCOE range for each of the nine test sites.

The linear relation of change in LCOE and FLH is logical, as irradiance influences yield and therefore, LCOE (cf. Eq. 3a). As the results indicate, the STD strategy performs worse compared to the NO strategy in most of the cases, and only exceptions occur as previously mentioned. In the few cases when the STD strategy performs better, the cost advantage is small. The biggest cost reduction could be found for Lappeenranta with 0.4%; however, the cost may as well be up to 8.7% and 9.0% higher in northern latitudes in Lappeenranta and Watson Lake, respectively, depending on the row spacing. The ADV strategy performs better for all row spacings compared to no backtracking; however, the cost advantage is also rather small for all test sites of up to 1.2% in LCOE in Munich. In some cases, the ADV strategy shows neither an improvement nor a deterioration. A clear cost improvement for all test sites can be noticed for the ADVS strategy. An at least  $-0.4\%$  LCOE deviation can be achieved for high row spacings in Ouarzazate and Tete, and an up to  $-5.0\%$  deviation in LCOE is possible in Munich. While these results prove the advantages or disadvantages of the backtracking strategies versus not applying backtracking, the same can be investigated compared to the STD strategy, which is done as well in Fig. 10.

Naturally, the economic performance of the NO strategy relative to the STD strategy shows the inverted results as when comparing the STD strategy to the NO strategy, though the absolute numbers change minorly due to the different calculation basis, which is now the STD strategy. The LCOEs of the NO strategy are up to 0.4% higher and can be as low as  $-8.3\%$  compared to the standard backtracking algorithm STD. Compared to this standard variant, the ADV strategy shows significant improvement as well. Only in Lappeenranta does the case occur where the ADV strategy shows higher LCOE of up to 0.2% for large row spacings. In all other cases, the ADV strategy performs better than the STD

strategy. The LCOE can be improved by up to 8.9% in Watson Lake, while in Lappeenranta an 8.5% decrease can be achieved. For large row spacings, the cost advantage vanishes at all test sites. However, for test sites with very good solar conditions (Ouarzazate, Kuala Lumpur, Tete), the minimum cost advantage still can be as much as 0.3% (Kuala Lumpur) to 0.7% (Ouarzazate). Most significant is the cost advantage of the ADVS strategy over the STD strategy. Due to its sophisticated algorithm of checking all possible tilt angles between the true tracking angle and  $0^\circ$ , an at least 0.6% cost reduction (Brasilia, Jaisalmer) can be achieved throughout all test sites and row spacings investigated. Test sites closer to the equator can improve their cost performance to about 5.0% for small row spacings. In detail, the maximum cost reduction is 4.6% (Kuala Lumpur), 4.8% (Jaisalmer), 5.6% (Brasilia), and 6.6% (Tete). For moderate latitudes, the cost improvement already increases to 7.3% (Munich), 8.0% (Ouarzazate), and 9.1% (Xilin Gol). The most significant effect of the ADVS strategy can be noticed for high latitude sites, with a cost improvement of up to 11.7% in Lappeenranta (Finland), and 12.0% in Watson Lake (Canada).

## 5. Discussion and research outlook

Long-term planning of energy systems must include the optimisation of energy technologies and their application. In the context of solar PV as the expected future leader in renewable energy sources, considering the various options for the technology, such as fixed tilted, single-axis tracking, 2-axis tracking, floating (on- and offshore), and vertical, is essential. As the results in this study show, the details matter as well. In this study, results suggest that the standard backtracking approach of always avoiding mutual shading, while being the most straight-forward, is not necessarily the best solution in terms of techno-economic optimisation. A limitation of the present economic assessment are module degradation [50,51] and solar brightening effects [47], though their implementation in evaluations of the economic performance of solar PV is not yet standard in techno-economic modelling, similar to estimating a maximum lifetime [52]. Nevertheless, considering these effects should become standard in upcoming solar PV modelling research.

Even though different backtracking or irradiance optimisation strategies are not yet comprehensively discussed in literature, solar PV simulation software already offer these options. For example, PVsyst

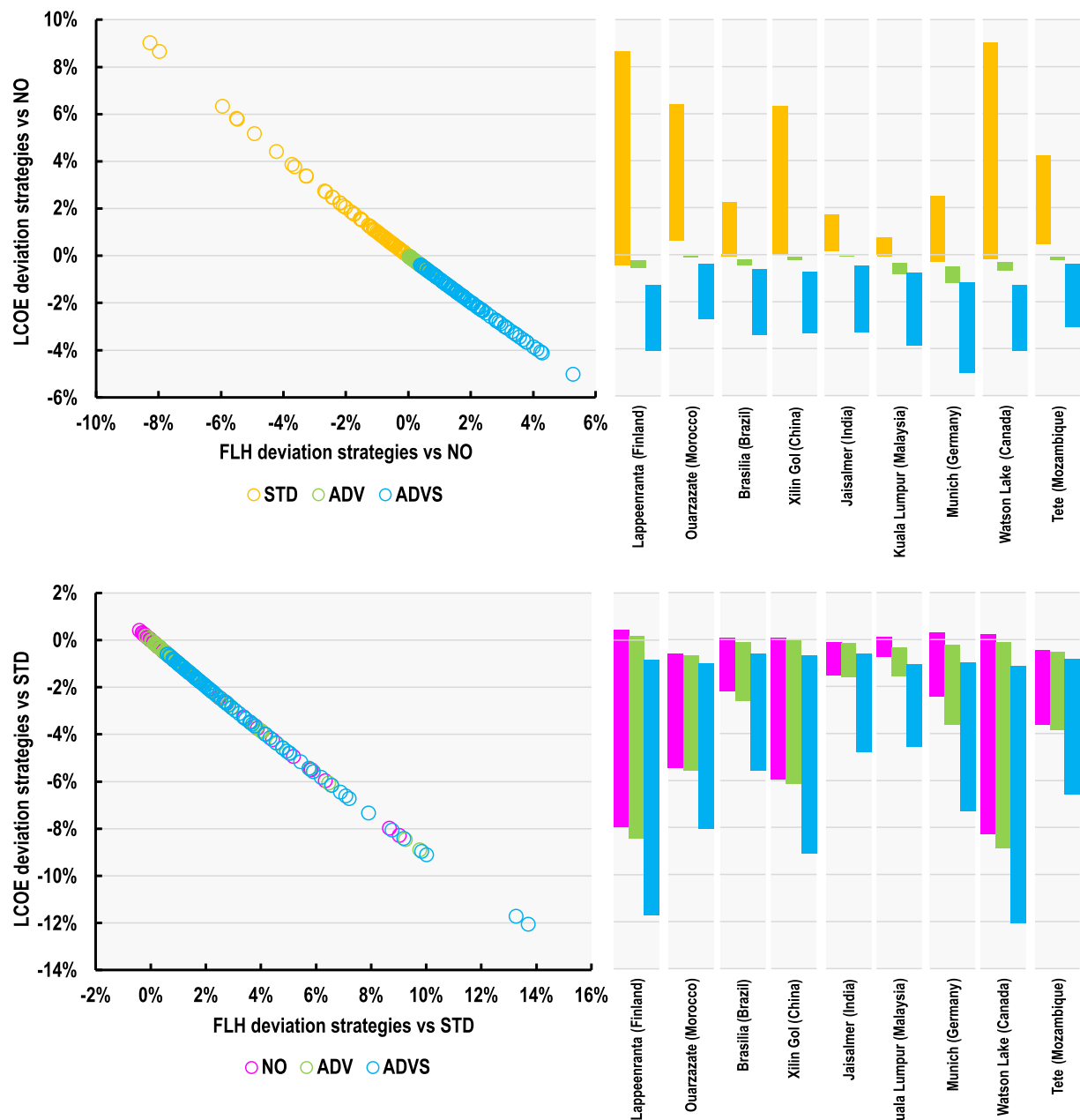


Fig. 10. Deviation of LCOE in 2025 of the STD, ADV, and ADVS strategies relative to the NO strategy (top) and deviation of LCOE in 2025 of the NO, ADV, and ADVS strategies relative to the STD strategy (bottom) over relative deviation of the FLH. Please note the different x-axis scaling. The columns on the right show the range of the relative LCOE for each of the test sites summarised over all investigated row spacings.

[41] offers two options for *backtracking* and *irradiance optimisation*; however, a detailed explanation on how the two strategies are implemented in detail is not available. Therefore, the *backtracking* option must be presumed to be equal or similar to the STD strategy presented in this study, and the *irradiance optimisation* option is equal or similar to the ADVS strategy.

In general, the results presented in this study are in line with the main outcomes of some of the studies presented in the literature review. Similar to Ngan et al. [29], the results show that backtracking, at least the standard strategy, might not always be the superior option. In most cases, true tracking or the NO strategy could outperform the STD strategy. As shown by Passow et al. [27] and Dolan et al. [28], the module type and cell type or technology are important factors to consider, as the present study accentuates. Most interesting are the results presented by Nicoletti et al. [25], since bifacial modules can be expected to grow significantly in the coming years and are expected to cover about 70 % [53,54] to 80 % [19] of the solar PV market by 2030. The global impact of different backtracking strategies on bifacial modules compared to monofacial modules should be emphasised in future research.

The present research uses the approach of hour-by-hour simulation. To allow for a smart implementation in real-life projects, a more sophisticated computation approach could be developed. As an example, Casares de la Torre et al. [55] applied a pool of equations for the determination of backtracking on the case of agrivoltaics. Barbón et al. [56] investigated the influence of the terrain slope on the tracker performance. A more general example is the study by Fernández-Ahumada et al. [57], who deducted generic equations for the tracking angle. The improved computation time of equation-based solutions over simulation-based solutions will be relevant to improve the tracker performance when applying the theory of this research in real-world projects.

One important issue is the application and technical realisation of the strategies, especially of the ADVS strategy, in real-world projects. Apart from difficult, hilly, and uneven terrains, the optimisation of the tilt angle could be realised using a few sensors on test rows of the whole power plant, feeding irradiance and sun angle information to a workstation or server. Using information on the setup of the power plant, the optimal tilt angle can be obtained theoretically in a relatively simple way.

Besides half cells, other cell aspect ratios such as third or quarter cells are on the rise [19]. Applying the same logic as used for Fig. 1, based on estimations provided by VDMA [20] it, third or quarter cells can be expected to make up to about 25% of the global utility-scale solar PV market by 2030, fully pushing full cells out of the market. Third or quarter cells in combination with HSATs can be estimated to have a share of about 10% by 2030 of the total installed utility-scale solar PV capacity. Depending on the string layout of the cells in the module, the importance of choosing the right backtracking strategy is equal or higher than for half cells.

## 6. Conclusions

This study assessed the impact of different backtracking strategies on the techno-economic performance of horizontal single-axis tracking solar photovoltaic power plants using state-of-the-art half cell modules. As a general reference, the performance of the artificial power plant has been simulated without applying a backtracking strategy. This reference case has been used to validate the LUT-PV model with the PVsyst software. Furthermore, three different backtracking strategies have been studied: Standard backtracking always avoiding mutual shading of the

tracker rows, advanced backtracking only applying backtracking if the total irradiation on the modules for a reduced tracking angle is favourable, and advanced sophisticated backtracking calculating the total irradiance on the modules for each of the possible tracking angles between the true tracking angle and a horizontal orientation and choosing the angle with the highest total irradiation. All strategies were studied for nine different test sites distributed all over the globe to cover different climatic conditions. In addition, the row spacing was varied to cover the impact of the backtracking strategies on area-optimised power plants.

The results indicate that the standard backtracking strategy is almost always outperformed by other backtracking strategies. Not applying backtracking and keeping the tracker at maximum tracking angles at times with low sun elevation was shown to be the superior strategy most of the time as well. Standard backtracking only showed an improved performance in high latitudes and wide row spacing. Compared to no backtracking, the full load hours of the power plant for the assessed test sites were generally lower for standard backtracking (−8.7% to 0.4%), about the same with tendency to higher full load hours for advanced backtracking (0.0% to 1.2%), and higher for advanced sophisticated backtracking (0.4% to 5.0%). Due to the linear relationship of yield, or full load hours, and levelised cost of electricity, the levelised costs of electricity of the standard backtracking strategy are up to 8.7% higher, the advanced strategy up to 1.2% lower for the advanced backtracking strategy, and up to 5.0% lower for the advanced sophisticated backtracking strategy. Compared to standard backtracking, the advanced backtracking strategy was able to outperform the standard backtracking with up to 8.9% higher yield and 8.9% lower levelised cost of electricity. The advanced sophisticated backtracking strategy achieved up to 12.0% higher full load hours and consequently, 12.0% lower levelised cost of electricity.

Solar photovoltaics becomes the leading renewable energy source in the decades to come. An optimal application of this technology, more specifically, horizontal single-axis tracking solar photovoltaic power plants, will only be possible if all aspects are considered. This study showed that backtracking is an important topic for single-axis tracking power plant planning. The results and limitations of the assessment were discussed and an outlook on future research opportunities provided.

## Declaration of competing interest

The authors declare that they have no known competing financial interests or personal relationships that could have appeared to influence the work reported in this paper.

## Acknowledgements

The authors gratefully acknowledge the public financing of European Union's Horizon 2020 research and innovation programme under grant agreement No 953016 (SERENDI-PV), which partly funded this research. Dominik Keiner would like to thank the Jenny and Antti Wihuri Foundation for the valuable grant. The authors would like to thank Gabriel Lopez for valuable proofreading.

## Appendix



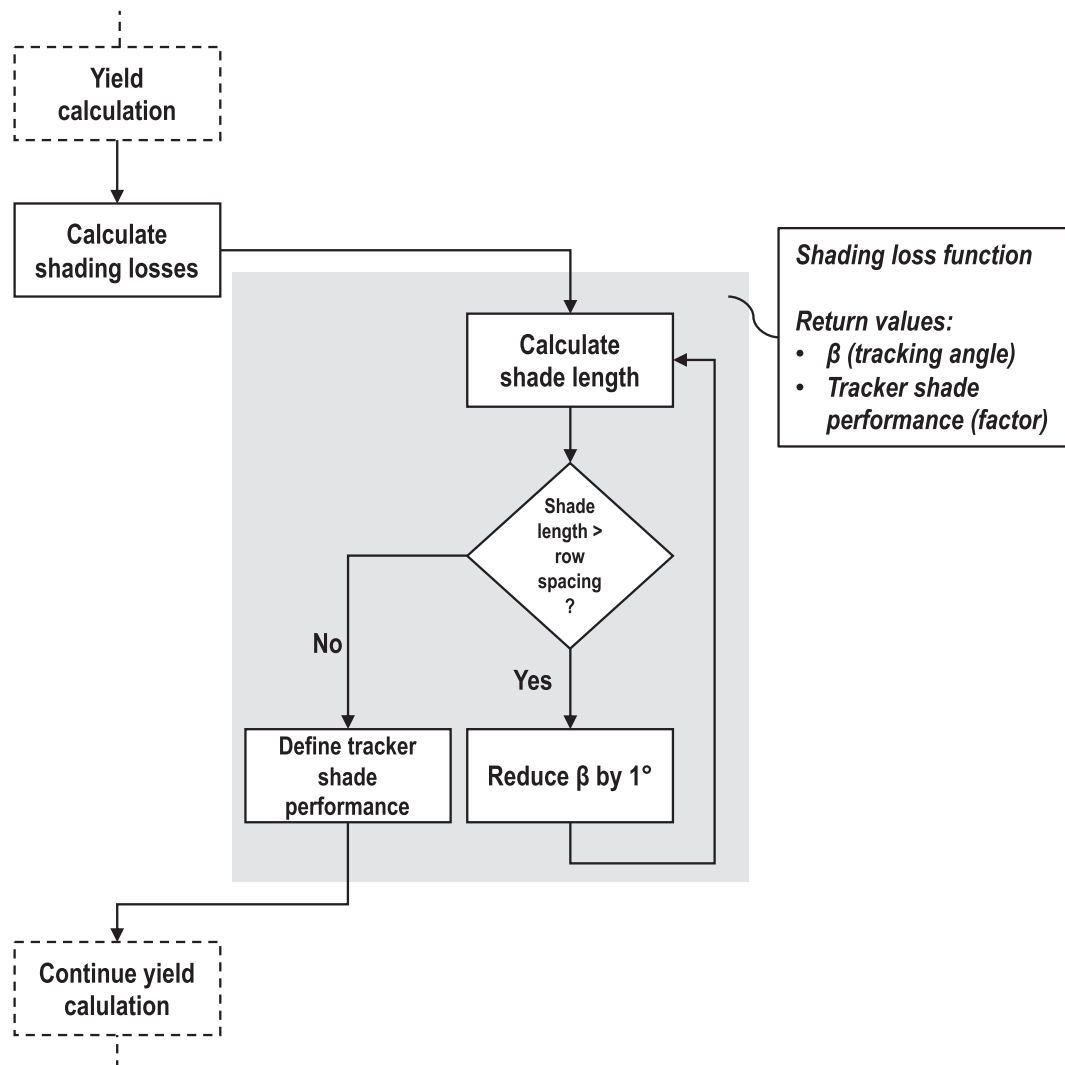


**Fig. A1.** Flow chart of the shading loss function as implemented for the STD strategy and embedded in the LUT-PV yield calculation. The shading loss function returns the new tracking angle  $\beta$  and a factor for the tracker shade performance (cf. Fig. 2).

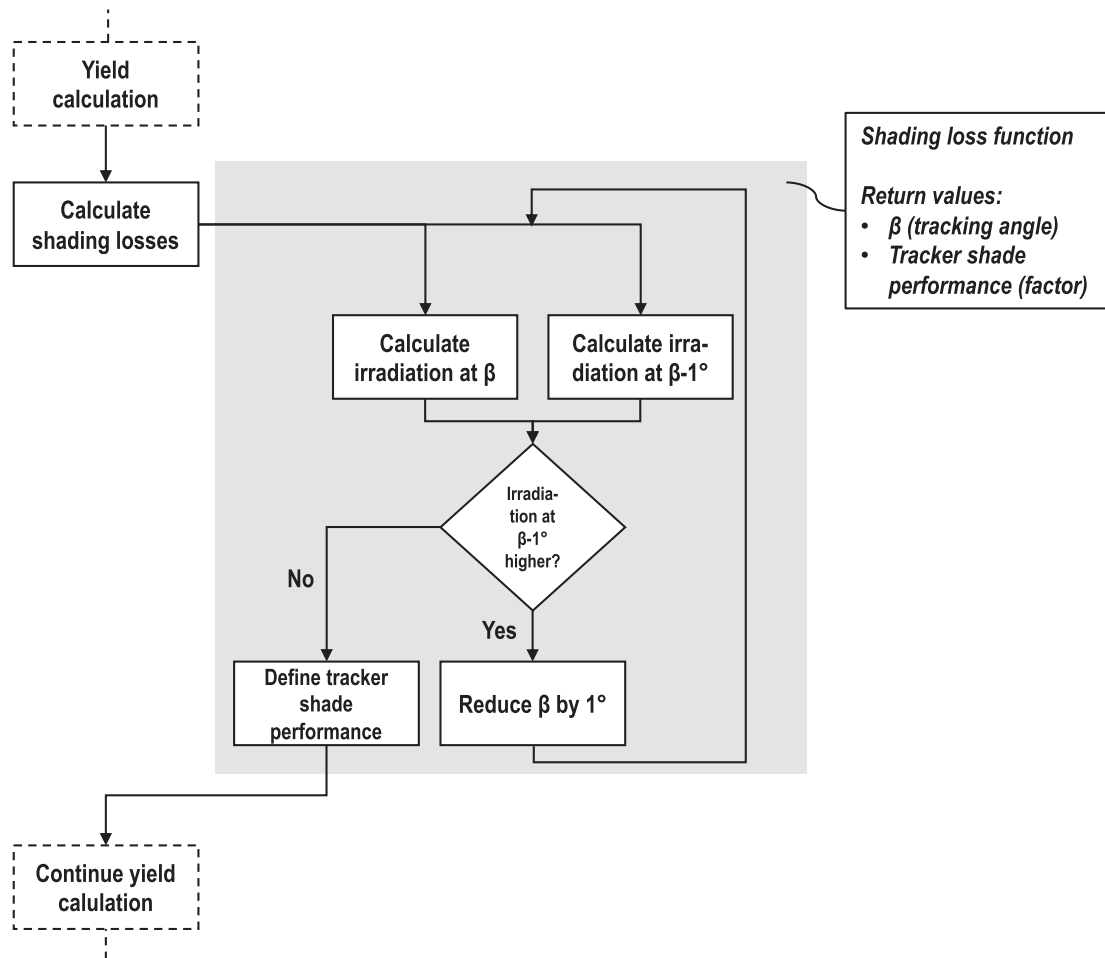


**Fig. A2.** Flow chart of the shading loss function as implemented for the ADV strategy and embedded in the LUT-PV yield calculation. The shading loss function returns the new tracking angle  $\beta$  and a factor for the tracker shade performance (cf. Fig. 2).

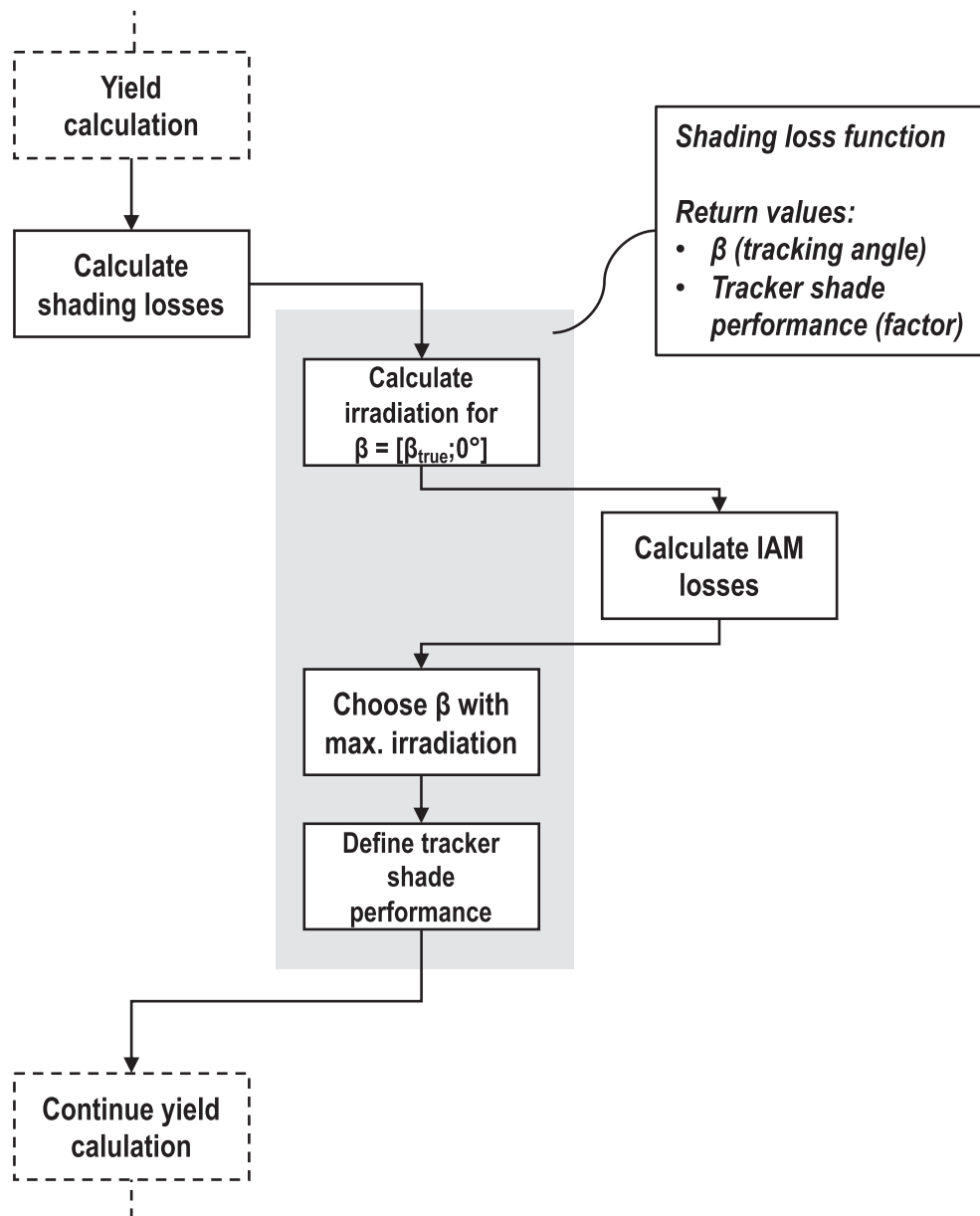


**Fig. A3.** Flow chart of the shading loss function as implemented for the ADVS strategy and embedded in the LUT-PV yield calculation.  $\beta_{true}$  is the true tracking angle. The function to calculate the IAM losses is an extern function, which is called at a later stage of the yield calculation again. The shading loss function returns the new tracking angle  $\beta$  and a factor for the tracker shade performance (cf. Fig. 2).

## Appendix A. Supplementary data

Supplementary data to this article can be found online at <https://doi.org/10.1016/j.solener.2023.112228>.

## References

- [1] IEA - International Energy Agency. World Energy Outlook 2020. Paris: 2020.
- [2] Breyer C, Bogdanov D, Khalili S, Keiner D. Solar Photovoltaics in 100% Renewable Energy Systems. In: Meyers RA, editor. Encyclopedia of Sustainability Science and Technology, New York, NY: Springer New York; 2021, p. 1–30. [https://doi.org/10.1007/978-1-4939-2493-6\\_1071-1](https://doi.org/10.1007/978-1-4939-2493-6_1071-1).
- [3] N.M. Haegel, P. Verlinden, M. Victoria, P. Altermatt, H. Atwater, T. Barnes, et al., Photovoltaics at multi-terawatt scale: waiting is not an option, Science 380 (2023) 39–42, <https://doi.org/10.1126/science.adf6957>.
- [4] M. Victoria, N. Haegel, I.M. Peters, R. Sinton, A. Jäger-Waldau, C. del Cañizo, et al., Solar photovoltaics is ready to power a sustainable future, Joule 5 (2021) 1041–1056, <https://doi.org/10.1016/j.joule.2021.03.005>.
- [5] S. Rachalra, K. Rajan, Solar tracking system - a review, Int. J. Sustain. Eng. 10 (2017) 72–81, <https://doi.org/10.1080/19397038.2016.1267816>.
- [6] O. Papathanasiou, M. Schmela, Market survey solar trackers 2021, Taiyang News (2021).
- [7] VDMA-Verband Deutscher Maschinen- und Anlagenbau e.V. International Technology Roadmap for Photovoltaic (ITRPV) - 2019 results. Frankfurt Am Main: 2020.
- [8] D. Bogdanov, M. Ram, A. Aghahosseini, A. Gulagi, A.S. Oyewo, M. Child, et al., Low-cost renewable electricity as the key driver of the global energy transition towards sustainability, Energy 227 (2021), 120467, <https://doi.org/10.1016/j.energy.2021.120467>.
- [9] S. Afanasyeva, D. Bogdanov, C. Breyer, Relevance of PV with single-axis tracking for energy scenarios, Sol. Energy 173 (2018) 173–191, <https://doi.org/10.1016/j.solener.2018.07.029>.
- [10] J. Antonanzas, R. Urraca, F.J. Martinez-de-Pison, F. Antonanzas, Optimal solar tracking strategy to increase irradiance in the plane of array under cloudy

- conditions: a study across Europe, *Sol. Energy* 163 (2018) 122–130, <https://doi.org/10.1016/j.solener.2018.01.080>.
- [11] P.H.A. Verissimo, R.A. Campos, M.V. Guarneri, J.P.A. Verissimo, L.R. Nascimento, do, R. Rüther R., Area and LCOE considerations in utility-scale, single-axis tracking PV power plant topology optimization, *Sol. Energy* 211 (2020) 433–445, <https://doi.org/10.1016/j.solener.2020.09.070>.
  - [12] N. Kutybay, A. Saymbetov, S. Mekhilef, M. Nurgaliyev, D. Tukymbekov, G. Dosymbetova, et al., Optimized single-axis schedule solar tracker in different weather conditions, *Energies* 13 (2020) 5226, <https://doi.org/10.3390/en13195226>.
  - [13] Y. Zhu, J. Liu, X. Yang, Design and performance analysis of a solar tracking system with a novel single-axis tracking structure to maximize energy collection, *Appl. Energy* 264 (2020), 114647, <https://doi.org/10.1016/j.apenergy.2020.114647>.
  - [14] M.T. Patel, M.S. Ahmed, H. Imran, N.Z. Butt, M.R. Khan, M.A. Alam, Global analysis of next-generation utility-scale PV: tracking bifacial solar farms, *Appl. Energy* 290 (2021), 116478, <https://doi.org/10.1016/j.apenergy.2021.116478>.
  - [15] C.D. Rodríguez-Gallegos, O. Gandhi, S.K. Panda, T. Reindl, On the PV tracker performance: tracking the sun versus tracking the best orientation, *IEEE J. Photovoltaics* 10 (2020) 1474–1480, <https://doi.org/10.1109/JPHOTOV.2020.3006994>.
  - [16] C.D. Rodríguez-Gallegos, H. Liu, O. Gandhi, J.P. Singh, V. Krishnamurthy, A. Kumar, et al., Global techno-economic performance of bifacial and tracking photovoltaic systems, *Joule* 4 (2020) 1514–1541, <https://doi.org/10.1016/j.joule.2020.05.005>.
  - [17] M.Z. Jacobson, M.A. Delucchi, M.A. Cameron, S.J. Coughlin, C.A. Hay, I. P. Manogaran, et al., Impacts of green new deal energy plans on grid stability, costs, jobs, health, and climate in 143 countries, *One Earth* 1 (2019) 449–463, <https://doi.org/10.1016/j.oneear.2019.12.003>.
  - [18] B. Lu, A. Blakers, M. Stocks, C. Cheng, A. Nadolny, A zero-carbon, reliable and affordable energy future in Australia, *Energy* 220 (2021), 119678, <https://doi.org/10.1016/j.energy.2020.119678>.
  - [19] VDMA-Verband Deutscher Maschinen- und Anlagenbau e.V. International Technology Roadmap for Photovoltaic (ITRPV) - 2021 results. Frankfurt Am Main: 2022.
  - [20] VDMA-Verband Deutscher Maschinen- und Anlagenbau e.V. International Technology Roadmap for Photovoltaic (ITRPV) - 2022 results. Frankfurt Am Main: 2023.
  - [21] E. Lorenzo, L. Narvarte, J. Muñoz, Tracking and back-tracking, *Prog. Photovolt. Res. Appl.* 19 (2011) 747–753, <https://doi.org/10.1002/pip.1085>.
  - [22] Panico D, Garvison P, Wenger H, Shugar D. Backtracking: a novel strategy for tracking PV systems. The Conference Record of the Twenty-Second IEEE Photovoltaic Specialists Conference - 1991, IEEE; 1991, p. 668–73. <https://doi.org/10.1109/PVSC.1991.169294>.
  - [23] L.M. Fernández-Ahumada, J. Ramírez-Faz, R. López-Luque, M. Varo-Martínez, I. M. Moreno-García, F.C. de la Torre, Influence of the design variables of photovoltaic plants with two-axis solar tracking on the optimization of the tracking and backtracking trajectory, *Sol. Energy* 208 (2020) 89–100, <https://doi.org/10.1016/j.solener.2020.07.063>.
  - [24] M. Silva, R. Castro, M. Batalha, Technical and economic optimal solutions for utility-scale solar photovoltaic parks, *Electronics* 9 (2020) 400, <https://doi.org/10.3390/electronics9030400>.
  - [25] F. Nicoletti, M.A. Cucumo, V. Ferraro, D. Kaliakatos, J. Settino, Performance analysis of a double-sided PV plant oriented with backtracking system, *Mathematical Modelling of Engineering Problems* 7 (2020) 325–334, <https://doi.org/10.18280/mmep.070301>.
  - [26] A.K. Maximizing, Yield with Improved Single-Axis Backtracking on Cross-Axis Slopes 47th IEEE Photovoltaic Specialists Conference (PVSC), IEEE 2020 (2020) 1466–1471, <https://doi.org/10.1109/PVSC45281.2020.9300438>.
  - [27] K. Passow, J. Falls, K. Hunt, Sensitivity of PV Plant Performance to Tracker Error. IEEE 46th Photovoltaic Specialists Conference (PVSC), IEEE 2019 (2019) 0659–0662, <https://doi.org/10.1109/PVSC40753.2019.8980662>.
  - [28] D.S.L. Dolan, V. Prodanov, P. Salter, F. Cheein, J. Dolan, Reducing Performance Loss Due to Backtracking Error Through Use of Half Cut Cell Modules, in: 2019 9th International Conference on Power and Energy Systems (ICPES), IEEE, 2019, pp. 1–4, <https://doi.org/10.1109/ICPES47639.2019.9105393>.
  - [29] L. Ngan, C. Jepson, A. Blekicky, A. Panchula, Increased energy production of First Solar horizontal single-axis tracking PV systems without backtracking. IEEE 39th Photovoltaic Specialists Conference (PVSC), IEEE 2013 (2013) 0792–0796, <https://doi.org/10.1109/PVSC.2013.6744267>.
  - [30] D. Schneider, Control algorithms for large-scale single-axis photovoltaic trackers, *Acta Polytechnica* (2012) 52. <https://doi.org/10.14311/1648>.
  - [31] N. Inc, NX Gemini, Fremont, CA, 2023.
  - [32] Longi Solar. Hi-MO 4 LR4-72HPH 430 460M data sheet. 2020.
  - [33] Sineng Electric Co., Ltd. PV Inverter 2021. <https://en.si-neng.com/> (accessed March 1, 2023).
  - [34] H.X. Wang, M.A. Muñoz-García, G.P. Moreda, M.C. Alonso-García, Optimum inverter sizing of grid-connected photovoltaic systems based on energetic and economic considerations, *Renew. Energy* 118 (2018) 709–717, <https://doi.org/10.1016/j.renene.2017.11.063>.
  - [35] Stackhouse P, Whitlock C. Surface meteorology and solar energy (SSE) release 6.0, NASA SSE 6.0. [https://searchworks.stanford.edu/catalog?q=%2522NASA%2bLangley%2bAtmospheric%2bSciences%2bData%2bCenter%2522%26search\\_field=search\\_author](https://searchworks.stanford.edu/catalog?q=%2522NASA%2bLangley%2bAtmospheric%2bSciences%2bData%2bCenter%2522%26search_field=search_author), Langley: 2008.
  - [36] Stackhouse P, Whitlock C. Surface meteorology and solar energy (SSE) release 6.0 Methodology, NASA SSE 6.0. <https://power.larc.nasa.gov/docs/methodology/>, Langley: 2009.
  - [37] D. Stetter, Enhancement of the REMix energy system model: global renewable energy potentials, optimized power plant siting and scenario validation, University of Stuttgart, 2012. PhD thesis, Faculty of energy-, process- and bio-engineering..
  - [38] M. Akhasssi, A.E. Fathi, N. Erraissi, N. Aarich, A. Bennouna, M. Raoufi, et al., Experimental investigation and modeling of the thermal behavior of a solar PV module, *Sol. Energy Mater. Sol. Cells* 180 (2018) 271–279, <https://doi.org/10.1016/j.solmat.2017.06.052>.
  - [39] G.H. Yordanov, Relative efficiency revealed: equations for k1–k6 of the PVGIS model IEEE 40th Photovoltaic Specialist Conference (PVSC), IEEE 2014 (2014) 1393–1398, <https://doi.org/10.1109/PVSC.2014.6925178>.
  - [40] F. Martínez-Moreno, J. Muñoz, E. Lorenzo, Experimental model to estimate shading losses on PV arrays, *Sol. Energy Mater. Sol. Cells* 94 (2010) 2298–2303, <https://doi.org/10.1016/j.solmat.2010.07.029>.
  - [41] PVSyst SA. PVSyst 2023. <https://pvsyst.com/> (accessed March 3, 2023).
  - [42] C3S - Copernicus Climate Change Service. ERA5-Land hourly data from 2001 to present 2019. <https://doi.org/10.24381/CDS.E2161BAC>.
  - [43] Jerue R. Köppen-Geiger Climate Classification 2021. <https://www.koppen-map.com/> (accessed March 3, 2023).
  - [44] M. Kottek, J. Grieser, C. Beck, B. Rudolf, F. Rubel, World Map of the Köppen-Geiger climate classification updated, *Meteorol. Z.* 15 (2006) 259–263, <https://doi.org/10.1127/0941-2948/2006/0130>.
  - [45] S. Hercege, I. Kaaya, J. Ascencio-Vásquez, M. Fischer, K.-A. Weiß, L. Schebek, The influence of different degradation characteristics on the greenhouse gas emissions of silicon photovoltaics: a threefold analysis, *Sustainability* 14 (2022) 5843, <https://doi.org/10.3390/su14105843>.
  - [46] D.C. Jordan, S.R. Kurtz, K. VanSant, J. Newmiller, Compendium of photovoltaic degradation rates, *Prog. Photovolt.* 24 (2016) 978–989, <https://doi.org/10.1002/pip.2744>.
  - [47] M. Wild, Global dimming and brightening: A review. *J. Geophys. Res.* 2009;114: 2008JD011470. <https://doi.org/10.1029/2008JD011470>.
  - [48] M. Wild, D. Folini, M.Z. Hakuba, C. Schär, S.I. Seneviratne, S. Kato, et al., The energy balance over land and oceans: an assessment based on direct observations and CMIP5 climate models, *Clim. Dyn.* 44 (2015) 3393–3429, <https://doi.org/10.1007/s00382-014-2430-z>.
  - [49] S. Fuzzi, U. Baltensperger, K. Carslaw, S. Decesari, H. Denier Van Der Gon, M. C. Facchini, et al., Particulate matter, air quality and climate: lessons learned and future needs, *Atmos. Chem Phys* 15 (2015) 8217–8299, <https://doi.org/10.5194/acp-15-8217-2015>.
  - [50] L. Koester, S. Lindig, A. Louwen, A. Astigarraga, G. Manzolini, D. Moser, Review of photovoltaic module degradation, field inspection techniques and techno-economic assessment, *Renew. Sustain. Energy Rev.* 165 (2022), 112616, <https://doi.org/10.1016/j.rser.2022.112616>.
  - [51] M. Aghaei, A. Fairbrother, A. Gok, S. Ahmad, S. Kazim, K. Lobato, et al., Review of degradation and failure phenomena in photovoltaic modules, *Renew. Sustain. Energy Rev.* 159 (2022), 112160, <https://doi.org/10.1016/j.rser.2022.112160>.
  - [52] I.M. Peters, J. Hauch, C. Brabec, P. Sinha, The value of stability in photovoltaics, *Joule* 5 (2021) 3137–3153, <https://doi.org/10.1016/j.joule.2021.10.019>.
  - [53] R. Kopecek, J. Libal, Bifacial photovoltaics 2021: status, opportunities and challenges, *Energies* 14 (2021) 2076, <https://doi.org/10.3390/en14082076>.
  - [54] R. Kopecek, J. Libal, Towards large-scale deployment of bifacial photovoltaics, *Nat. Energy* 3 (2018) 443–446, <https://doi.org/10.1038/s41560-018-0178-0>.
  - [55] F.J. Casares De La Torre, M. Varo, R. López-Luque, J. Ramírez-Faz, L.M. Fernández-Ahumada, Design and analysis of a tracking / backtracking strategy for PV plants with horizontal trackers after their conversion to agrivoltaic plants, *Renew. Energy* 187 (2022) 537–550, <https://doi.org/10.1016/j.renene.2022.01.081>.
  - [56] A. Barbón, P. Fortuny Ayuso, L. Bayón, C.A. Silva, Experimental and numerical investigation of the influence of terrain slope on the performance of single-axis trackers, *Appl. Energy* 348 (2023), 121524, <https://doi.org/10.1016/j.apenergy.2023.121524>.
  - [57] L.M. Fernández-Ahumada, F.J. Casares, J. Ramírez-Faz, R. López-Luque, Mathematical study of the movement of solar tracking systems based on rational models, *Sol. Energy* 150 (2017) 20–29, <https://doi.org/10.1016/j.solener.2017.04.006>.